Ferroelectric Phase Transition Driven by Switchable Covalent Bonds

Han-Yue Zhang,[1,*] Nan Zhang,[1] Yao Zhang,[1] Huan-Huan Jiang,[1] Yu-Ling Zeng,[2] Shu-Yu Tang,[2] Peng-Fei Li,[2] Yuan-Yuan Tang,[2] and Ren-Gen Xiong[1,†]

[1]*Jiangsu Key Laboratory for Biomaterials and Devices, State Key Laboratory of Bioelectronics, School of Biological Science and Medical Engineering, Southeast University, Nanjing 210096, People's Republic of China*

[2]*Ordered Matter Science Research Center, Nanchang University, Nanchang 330031, People's Republic of China*

(Received 10 October 2022; accepted 5 April 2023; published 28 April 2023)

The mechanism on ferroelectric phase transitions is mainly attributed to the displacive and/or order-disorder transition of internal components since the discovery of the ferroelectricity in 1920, rather than the breaking and recombination of chemical bonds. Here, we demonstrate how to utilize the chemical bond rearrangement in a diarylethene-based crystal to realize the light-driven *mm*2F1-type ferroelectric phase transition. Such a photoinduced phase transition is entirely driven by switchable covalent bonds with breaking and reformation, enabling the reversible light-controllable ferroelectric polarization switching, dielectric and nonlinear optical bistability. Moreover, light as quantized energy can achieve contactless, nondestructive, and remote-control operations. This work proposes a new mechanism of ferroelectric phase transition, and highlights the significance of photochromic molecules in designing new ferroelectrics for photocontrol data storage and sensing.

DOI: 10.1103/PhysRevLett.130.176802

Diarylethenes with heterocyclic aryl groups have been considered to be one of the most promising photoresponsive materials with light-control tautomerism between open- and closed-ring isomers [1,2]. Different from traditional *T*-type (thermally reversible) photochromic molecules such as azobenzene, spiropyran, and salicylideneaniline [3–5], diarylethenes classified into *P* type (thermally irreversible, but photochemically reversible) have the striking features of thermal stability of both isomers, high sensitivity, rapid response, and fatigue resistance [6–8], which are essential and indispensable for various applications of photochromic molecules in optical memories, switches, and molecular machines [9–12]. It should be emphasized that such photoisomerization involved chemical bond rearrangement, with high photoexcitation conversion efficiency up to 100% and solid-phase reactivity [1], can effectively drive reversible structural phase transitions in the crystalline state. The structural phase transition associated with broken spatial-inversion symmetry is important for numerous physical systems [13–19], particularly for ferroelectrics that require polar symmetry for spontaneous polarization. In terms of the thermodynamic phase transition, the ferroelectric mechanisms are generally attributed to order-disorder and displacive transitions of internal components [20–30], rather than breaking and reorganization of chemical bonds. Notably, the ferroic phase transition involving switchable coordination bonds (N—O—K and C—F—K) have been reported in some molecular crystals represented by $[(CH_3)_3NOH]_2[KFe(CN)_6]$ [31–35]. However, such type of switchable coordination bonds is actually a change in the distance between the coordinating atoms caused by the order-disorder transition of the guest cations. The main mechanism of these structural phase transitions is still due to order-disorder transition of components. To date, harnessing new mechanisms of structural phase transitions driven entirely by true switchable covalent bonds with breaking and reformation for molecular ferroelectrics has been a daunting task.

Here, we present the covalent bond-switching process in a photochromic organic crystal, 1,2-bis(2-methyl-5-(4-pyridyl)-3-thienyl)perfluorocyclopentene (DTh-Py) [36], where the photoinduced switchable covalent bonds drive a ferroelectric structural phase transition with the Aizu notation of *mm*2F1 [40]. Under photoirradiation, its spontaneous polarization can be switched reversibly between two polar phases with the respective open-ring and closed-ring forms triggered by structural photoisomerizations with covalent bond-switching process (Fig. 1). Actually, we have reported a series of salicylideneaniline-based organic ferroelectrics and a pair of enantiomorphic diarylethene derivative ferroelectrics [41–46]. In these articles, however, we only observed the experimental phenomena of light-driven polarization switching, such as the transition between the enol and *trans*-keto forms of the Schiff base derivatives and the open- and closed-ring structural isomerization of diarylethene derivatives, where the rearrangement of covalent bonds was never mentioned. Based on the discovery of this new physical phenomenon in these articles, we summarize and first propose a new ferroelectric phase transition mechanism of covalent bond-switching in this work, which is entirely driven by intramolecular switchable covalent bonds with breaking and reformation, enabling the reversibly

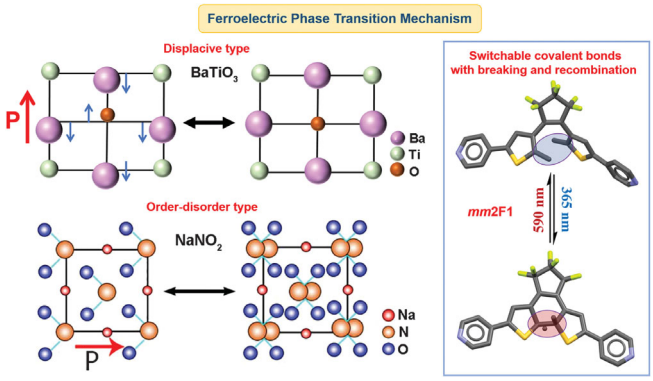

FIG. 1. Schematic illustrations of the ferroelectric mechanism for the displacive-type, order−disorder-type, and the new type with switchable covalent bonds (breaking and recombination). Many inorganic oxides such as $BaTiO_3$ belong to the displacive type, in which relative displacement of the ions causes the phase transition. $NaNO_2$ is a typical ferroelectric of order-disorder type, in which reorientation of the dipolar NO_2 ions induces ferroelectric phase transition. The ferroelectric structural phase transition in DTh-Py is driven by the photoinduced switchable covalent bonds.

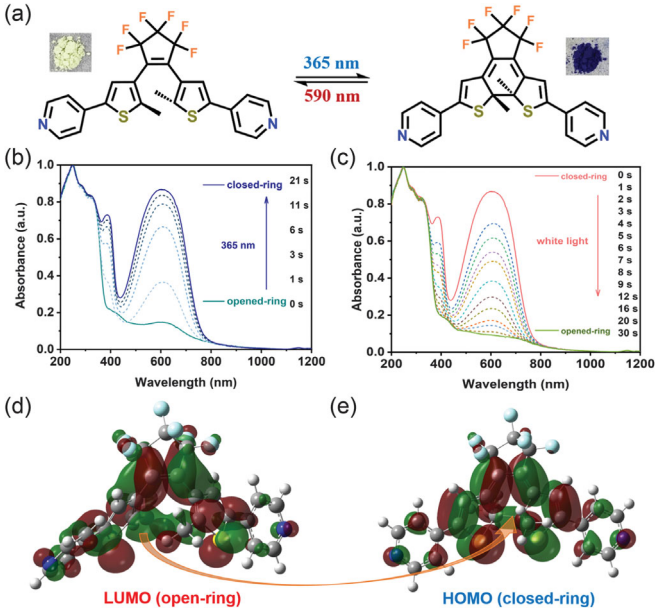

FIG. 2. (a) The molecular structures of DTh-Py and photomicrographs of the polycrystalline sample under alternating UV and visible light irradiation. Variation diagram of UV absorption curves under the light radiation of (b) 365 and (c) 590 nm. Theoretical interpretation of the photoisomerization process: (c) LUMO of open-ring form and (d) HOMO of a closed-ring form.

light-controllable ferroelectric polarization switching, dielectric and nonlinear optical bistability. This new ferroelectric phase transition mechanism would open up a new field of ferroelectrics, providing a new avenue for designing advanced photoresponsive ferroelectric materials for photocontrol computing and memory.

Single crystal samples of DTh-Py were prepared by slow evaporation from a saturated solution of its precursor materials, and its synthetic procedures are described in detail in the supporting information. The photoisomerization processes of diarylethene organic systems are generally accompanied by obvious photochromic behaviors. Photochromic properties of DTh-Py were first investigated by recording solid-state UV-vis (ultraviolet-visible) spectra (Fig. 2). Under the visible light irradiation, the absorption range of DTh-Py is below 400 nm, in good accordance with its pale yellow appearance [Fig. 2(b)]. After UV irradiation at 365 nm, a new absorption band peaked at about 600 nm emerged with an absorption edge close to 800 nm, and the peak intensity gradually increases until saturation with the increased irradiation time. At the same time, the apparent color of DTh-Py sample changed from pale yellow to dark blue. In turn, when the sample was subsequently exposed to light irradiation of 590 nm, the intensity of the absorption peak at 600 nm gradually weakened to almost disappear, and returned to the initial state after 30 s of illumination [Fig. 2(c)]. The photochromic behavior of DTh-Py is attributed to the reversible isomerization between open-ring and closed-ring forms, accompanied by the breaking and recombination of covalent bonds between two thienyl groups [Fig. 2(a)]. Notably, DTh-Py is thermally stable in either form, and exhibits good thermal stability and cyclability as well as almost a 100% conversion rate of photoisomerization in the solid state.

Frontier molecular orbital theory can provide a deeper understanding of the electronic structure. The highest occupied molecular orbital (HOMO) and lowest unoccupied molecular orbital (LUMO) of DTh-Py molecules with open- and closed-ring forms are calculated. The photoisomerization of such ring-closure process can be understood as a photochemical reaction. When illuminated, one electron of the open-ring HOMO is excited to the LUMO. From the LUMO of the molecule [Fig. 2(d)], the orbitals of two adjacent carbon-carbon double (π) bonds share the same orbital phase and have already partially been overlapped, which meets the orbital phase symmetry requirement for the ring-closure reaction. When these two adjacent carbon atoms run toward each other, the orbitals are further overlapped, thereby forming a carbon-carbon single (σ) bond and completing the ring-closure reaction [Fig. 2(e)].

In order to demonstrate this photoisomerization process more intuitively, we selected the distance between adjacent carbon atoms as an independent variable and performed a relaxed PES (potential energy surface) scan of the whole process. As shown in Fig. S1a of the Supplemental Material [36], during the evolution from open- to closed-ring structure, the energy curve increases monotonically. See Movie S1 for the animation of such a dynamic process. We further performed geometric optimization on the closed-ring structure and found that its energy is

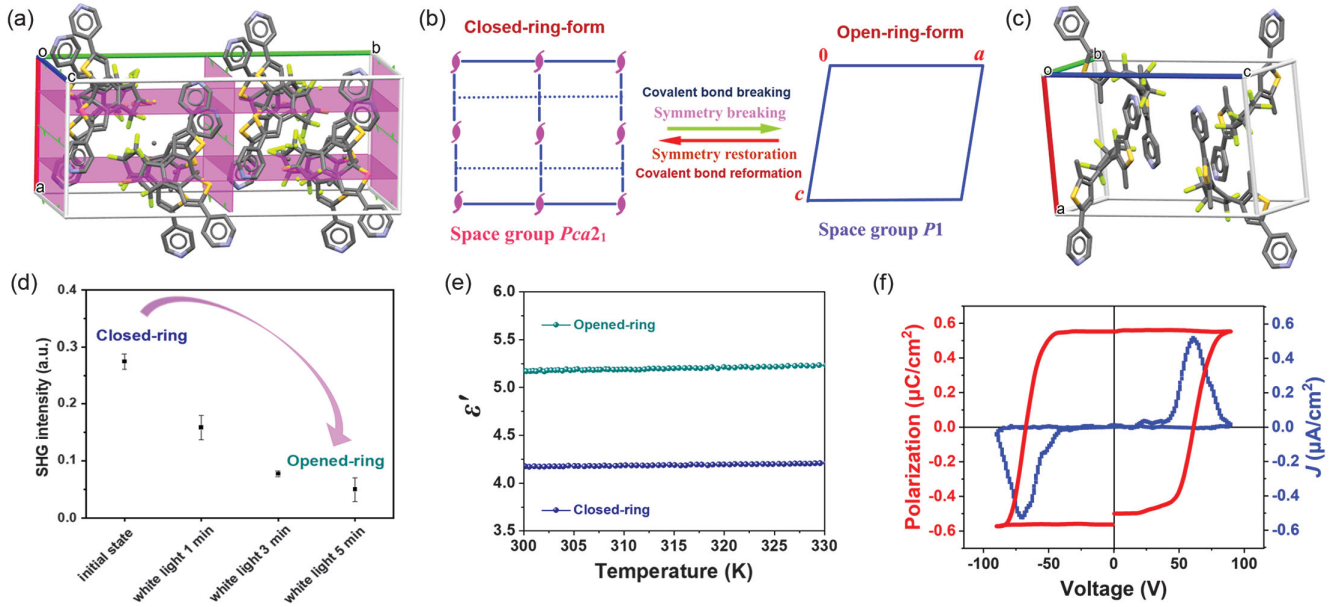

FIG. 3. Packing view of unit cell of the crystal structures for the (a) closed-ring form and (b) open-ring form, where hydrogen atoms are omitted for clarity. (c) Transformation of the space group of DTh-Py from the phases of closed-ring form to open-ring form. (d) Second harmonic generation (SHG) intensity and (e) dielectric constant of DTh-Py measured under alternating UV and visible light irradiation. (f) Polarization-voltage ($P-V$) hysteresis loop of DTh-Py with closed-ring form.

0.42 eV higher than that of the open-ring structure, and its dipole moment (2.56 D, Fig. S2) is smaller than that of the open-ring structure (2.73 D, Fig. S3). The difference in the electronic structure of the open- and closed-ring structures also leads to the huge difference in the spectra of two molecules. As shown in Fig. S1b, compared with the open-ring conformation, the closed-ring form displays new absorption peak centered at 617 nm, which can be attributed to the emergence of lower energy band due to more conjugated molecular structure. The different absorption spectra of open- and closed-ring molecules also means that the energy required for the conversion between them is different. Such interconversion can be illustrated as in Fig. S4 [36]. Therein, the open-ring configuration absorbs UV light at wavelengths less than ~400 nm to obtain relatively high energies to cross the transition energy barrier. Correspondingly, the closed-ring configuration only needs to absorb visible light to obtain sufficient energy to cross the energy barrier.

Single-crystal structure characterization by x-ray diffraction (XRD) reveals that DTh-Py with closed-ring form crystallizes in orthorhombic point group $mm2$ with a polar space group $Pca2_1$ (Table S1 [36]), which is ferroelectrically active in principle. Such crystal symmetry determines the direction of its spontaneous polarization along the [0 0 1] direction (along the c axis). The asymmetric unit of DTh-Py with closed-ring form consists of two molecules (Fig. S5), whose crystal structure is packed according to the symmetry elements of twofold screw axis along the c axis and two types of glide planes perpendicular to the a and b axes, respectively [Fig. 3(a)]. After photoisomerization to the open-ring form under light irradiation at 590 nm, the crystal undergoes a structural phase transition with the Aizu notation of $mm2F1$ [Fig. 3(b)]. The space group transforms into triclinic $P1$ with the lowest symmetry (Table S1 [36]), accompanied by the symmetry breaking with the loss of the twofold screw axis and glide planes, which allows ferroelectric polarization to have components in three all crystallographic axes of DTh-Py with open-ring form [Fig. 3(c)]. Correspondingly, the asymmetric unit contains four molecules with open-ring form (Fig. S6 [36]). Notably, DTh-Py was reported to crystallize in the centrosymmetric $P\bar{1}$ space group [47], but its obvious SHG signal response and piezoelectricity reveal its noncentrosymmetric characteristics with $P1$ space group. To obtain good refinement results, some carbon atoms and fluorine atoms in the molecules in the lattice of both isomers were split into two equivalent positions with a certain occupancy ratio, because of the large atomic thermal ellipsoid and displacement parameters. The good phase purity of the crystal samples has been verified by powder x-ray diffraction measurements (Fig. S7 [36]). Therefore, it is clear that such $mm2F1$-type ferroelectric phase transition mechanism is attributed to the covalent bond switching of organic molecules, which is triggered by the light stimulation of quantifiable energy and completely different from the conventional temperature-dependent ferroelectric phase transition.

Both phases of the DTh-Py crystal have polar symmetry, which means theoretically nonlinear optical response. The SHG effect has been widely used as an effective method to detect the breaking of the space-inversion symmetry [36]. As shown in Fig. S8, the SHG signals of both phases with

closed-ring and open-ring forms are active, while the SHG intensity of the former is about 6 times that of the latter and 1 order of magnitude smaller than that of KH_2PO_4 (KDP). When irradiating the visible light on the sample with closed-ring form, its SHG intensity decreases with increasing irradiation time until it becomes stable [Fig. 3(d)]. In addition to the changes in SHG response, DTh-Py exhibits bistability in dielectric properties as well. We measured the real part (ε') of dielectric permittivity in both phases. The ε' value of the phase with closed-ring form remains constant at about 5.2 from room temperature to around 330 K [Fig. 3(e)]. Under the UV light illumination with 365 nm, the ε' decreases from the initial value of 5.2 to about 4.2, and the value of ε' can return to the initial value after visible light irradiation. By alternating UV and visible light irradiation, DTh-Py can show the photoinduced bistable switching characteristics of dielectric permittivity and SHG response. Differential scanning calorimetry (DSC) analysis reflects that DTh-Py does not undergo a temperature-dependent structural phase transition (Fig. S9 [36]). The high melting point above 450 K endows DTh-Py with a wider operating temperature for ferroelectricity and other light-responsive switchable bistability. To investigate polarization switching behaviors, we measured the polarization-voltage ($P-V$) hysteresis loop on the thin film of DTh-Py with closed-ring form by using a double wave method [Fig. 3(f)]. The resulting $P-V$ hysteresis loop with a well-rectangular shape exhibits direct evidence of its ferroelectricity with a remanent polarization value of 0.55 $\mu C/cm^2$.

To more solidly determine its ferroelectric properties, we further performed the determination of microscale ferroelectric domain structure and switchable polarization behavior under different light irradiation. Piezoresponse force microscopy (PFM) can serve as an ideal tool to examine the ferroelectric behaviors via the visualization of domain structure and the polarization switching. The as-grown ferroelectric domains for DTh-Py thin film with closed-ring form were shown in Figs. 4(a) and 4(b), implying the existence of bistable polarization states. The domains exhibit an irregular profile, with domain walls that appear as dark lines in the amplitude image.

By definition, a ferroelectric material should possess spontaneous polarization that is switchable. To verify this, we scanned the initial as-grown state over an area of 10 μm × 10 μm in the DTh-Py thin film with closed-ring form [Fig. 4(d)], in which the region marked with a blue box was poled by a tip bias of +90 V. In the phase image, the domains indicated by the yellow color tone distinctly shrank, while the purple-colored domain expanded, suggesting a switching of the polarization state [Fig. 4(e)]. Then, by subsequent poling the same region with an opposing tip bias of −90 V, partial yellow domains were switched back, as shown in Fig. 4(f). Detailed topography and PFM amplitude information are given in Fig. S10 of the Supplemental Material [36]. During the electric poling, the morphology

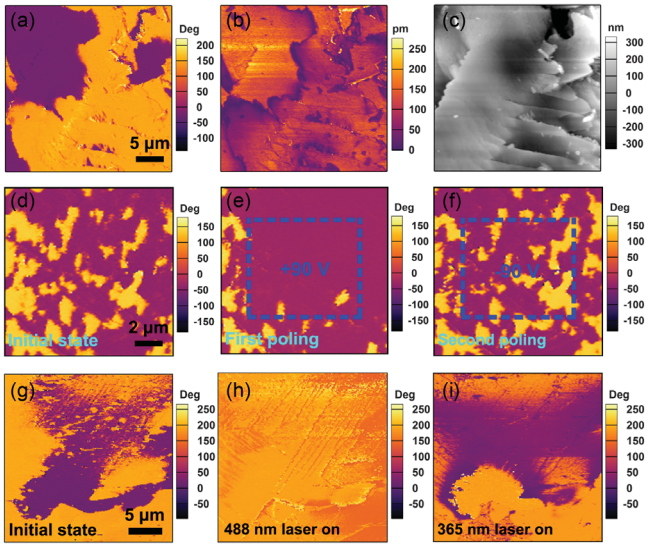

FIG. 4. Lateral PFM (a) phase, (b) amplitude and (c) corresponding topography images obtained in as-grown DTh-Py thin film with closed-ring form. Lateral PFM phase images of DTh-Py thin film with closed-ring form (d) at initial state, (e) after the first switching with a positive tip bias of +90 V over the blue box region, and (f) after the subsequent backswitching with a negative tip bias of −90 V over the same region. PFM phase images showing initial domain state measured in closed-ring sample (g) in dark, (h) after irradiating the sample with 488 nm laser for 5 s, and (i) after irradiating the sample with 365 nm laser for 1 min.

of the sample does not change and the domain walls can be discerned in the corresponding amplitude images, excluding the artifact imaging. To further confirm the polarization switching, the spectroscopic PFM measurements were performed on an arbitrary point in the thin film with closed-ring form. Then the sample surface is transformed into the open-ring state by illuminating with a 488 nm laser, and spectroscopic PFM measurements were performed *in situ* again. The acquired piezoresponse as a function of applied bias shows switchable hysteretic behavior, indicating that the polarization of DTh-Py with open-ring and closed-ring forms is switchable under an external bias (Fig. S11 [36]). These observations reveal that the polarization in DTh-Py thin film with closed-ring form is switchable under an external field, further confirming the material is ferroelectric.

It can be seen from the amplitude loops that the piezoresponse of the open-ring state is larger than that of the closed-ring state [Fig. S11(b)]. We further used PFM to measure the piezoresponse of DTh-Py thin film at both states *in situ*, by applying an ac voltage to excite the piezoelectric vibration of the sample. The principles and details of this method can be found in previous work [48]. In both states, the amplitude versus frequency curves fitted well with the SHO model [Fig. S12(a) [36]]. From Fig. S12(b), the slope of the measured vertical PFM amplitude vs drive voltage curves of the open-ring state is about 1.5 times that of the closed-ring state, corresponding to 1.5 times the magnitude of their piezoresponse.

PFM images as well as the corresponding topographic images taken before and after different laser irradiation of an initial thin film with closed-ring form are presented in Figs. 4(g), 4(h) and Fig. S13 of [36]. The original domain structure was measured in the dark, as shown in Fig. 4(g) and Figs. S13(a), S13(b). Figure 4(h) and S13(c), S13(d) show that a single domain state was obtained when the sample was illuminated by the 488 nm laser for 5 s. Then, by irradiating the same area with a 365 nm laser, we found that partial of the yellow domains were backswitched to purple domains [Fig. 4(i) and Figs. S13(e), S13(f)]. The surface morphology of the thin films did not change significantly during the laser irradiation (Fig. S13). These results demonstrate that reversible switching in DTh-Py can be achieved with a two color approach, whereby changing the wavelength of the incident light reverses the direction of the ferroelectric order parameter.

In summary, we reported a photochromic ferroelectric crystal, DTh-Py, which undergoes light-triggered structural phase transition driven entirely by covalent bond switching, accompanied by photoisomerization between the open-ring and closed-ring forms. Polarization-voltage hysteresis loop shows clear ferroelectricity with the remanent polarization of 0.55 $\mu C/cm^2$ for the closed-ring form of DTh-Py. Benefit from the reversible photoisomerization, the dielectric constant and SHG response can be reversibly switched by light. More strikingly, DTh-Py shows reversibly photoinduced ferroelectric polarization switching behavior, making it have great potential in applications for next-generation photocontrol ferroelectric data storage and sensing. This work presents a new ferroelectric phase transition mechanism of covalent bond switching, completely different from conventional ordered −disorder or displacement-type phases transition system, offering a new perspective for understanding the ferroelectric mechanism.

The manuscript was improved by the insightful reviews by the anonymous referees. This work was supported by the seventh Youth Elite Scientist Sponsorship Program by the China Association for Science and Technology, the Ten Science and Technology Problem of Southeast University, and the National Natural Science Foundation of China (No. 21991142 and No. 21831004).

*Corresponding author.
zhanghanyue@seu.edu.cn
†Corresponding author.
xiongrg@seu.edu.cn

[1] M. Irie, T. Fukaminato, K. Matsuda, and S. Kobatake, Chem. Rev. **114**, 12174 (2014).
[2] S. Kobatake, S. Takami, H. Muto, T. Ishikawa, and M. Irie, Nature (London) **446**, 778 (2007).
[3] E. Hadjoudis and I. M. Mavridis, Chem. Soc. Rev. **33**, 579 (2004).
[4] L. Kortekaas and W. R. Browne, Chem. Soc. Rev. **48**, 3406 (2019).
[5] Z. Mahimwalla, K. G. Yager, J.-i. Mamiya, A. Shishido, A. Priimagi, and C. J. Barrett, Polymer Bull. **69**, 967 (2012).
[6] M. Irie, Chem. Rev. **100**, 1685 (2000).
[7] M. Irie and M. Mohri, J. Org. Chem. **53**, 803 (1988).
[8] H. Tian and S. Yang, Chem. Soc. Rev. **33**, 85 (2004).
[9] D. Bleger and S. Hecht, Angew. Chem., Int. Ed. Engl. **54**, 11338 (2015).
[10] D. Kitagawa, H. Nishi, and S. Kobatake, Angew. Chem., Int. Ed. Engl. **52**, 9320 (2013).
[11] A. Perrier, F. Maurel, and D. Jacquemin, Acc. Chem. Res. **45**, 1173 (2012).
[12] J. Li, G. Speyer, and O. F. Sankey, Phys. Rev. Lett. **93**, 248302 (2004).
[13] W. Jin, E. Drueke, S. Li, A. Admasu, R. Owen, M. Day, K. Sun, S.-W. Cheong, and L. Zhao, Nat. Phys. **16**, 42 (2020).
[14] F. Li, Science **375**, 618 (2022).
[15] B. A. Strukov and A. P. Levanyuk, *Ferroelectric Phenomena in Crystals: Physical Foundations* (Springer Science & Business Media, New York, 2012).
[16] Y. Zhao and K. Zhu, Chem. Soc. Rev. **45**, 655 (2016).
[17] S. Horiuchi and Y. Tokura, Nat. Mater. **7**, 357 (2008).
[18] W. Li, Z. Wang, F. Deschler, S. Gao, R. H. Friend, and A. K. Cheetham, Nat. Rev. Mater. **2**, 16099 (2017).
[19] Y. Ai, R. Sun, W.-Q. Liao, X.-J. Song, Y.-Y. Tang, B.-W. Wang, Z.-M. Wang, S. Gao, and R.-G. Xiong, Angew. Chem., Int. Ed. **61**, e202206034 (2022).
[20] N. Dalal, A. Bussmann-Holder, and R. Blinc, *Ferro- and Antiferroelectricity: Order/Disorder Versus Displacive* (Springer, 2007).
[21] S. Kamba, APL Mater. **9**, 020704 (2021).
[22] M. Sepliarsky, M. G. Stachiotti, and R. L. Migoni, Phys. Rev. B **56**, 566 (1997).
[23] P. P. Shi, Y. Y. Tang, P. F. Li, W. Q. Liao, Z. X. Wang, Q. Ye, and R. G. Xiong, Chem. Soc. Rev. **45**, 3811 (2016).
[24] W. Zhang and R.-G. Xiong, Chem. Rev. **112**, 1163 (2012).
[25] O. Sato, Nat. Chem. **8**, 644 (2016).
[26] K. Iwano, Y. Shimoi, T. Miyamoto, D. Hata, M. Sotome, N. Kida, S. Horiuchi, and H. Okamoto, Phys. Rev. Lett. **118**, 107404 (2017).
[27] Y.-Y. Tang, P.-F. Li, P.-P. Shi, W.-Y. Zhang, Z.-X. Wang, Y.-M. You, H.-Y. Ye, T. Nakamura, and R.-G. Xiong, Phys. Rev. Lett. **119**, 207602 (2017).
[28] T. Akutagawa, H. Koshinaka, D. Sato, S. Takeda, S.-I. Noro, H. Takahashi, R. Kumai, Y. Tokura, and T. Nakamura, Nat. Mater. **8**, 342 (2009).
[29] H.-L. Cai, W. Zhang, J.-Z. Ge, Y. Zhang, K. Awaga, T. Nakamura, and R.-G. Xiong, Phys. Rev. Lett. **107**, 147601 (2011).
[30] H.-L. Cai, D.-W. Fu, Y. Zhang, W. Zhang, and R.-G. Xiong, Phys. Rev. Lett. **109**, 169601 (2012).
[31] X. G. Chen, Z. X. Zhang, Y. L. Zeng, S. Y. Tang, and R. G. Xiong, Chem. Commun. (Cambridge) **58**, 3059 (2022).
[32] M. Rok, A. Ciżman, B. Zarychta, J. K. Zaręba, M. Trzebiatowska, M. Mączka, A. Stroppa, S. Yuan, A. E. Phillips, and G. Bator, Phys. Rev. Lett. **109**, 169601 (2012).
[33] W.-J. Xu, P.-F. Li, Y.-Y. Tang, W.-X. Zhang, R.-G. Xiong, and X.-M. Chen, J. Am. Chem. Soc. **139**, 6369 (2017).

[34] W.-J. Xu, K. Romanyuk, Y. Zeng, A. Ushakov, V. Shur, A. Tselev, W.-X. Zhang, and X.-M. Chen, J. Mater. Chem. C **9**, 10741 (2021).
[35] W.-J. Xu, Y. Zeng, W. Yuan, W.-X. Zhang, and X.-M. Chen, Chem. Commun. (Cambridge) **56**, 10054 (2020).
[36] See Supplemental Material at http://link.aps.org/supplemental/10.1103/PhysRevLett.130.176802 for the sample syntheses and SHG measurements, which includes Refs. [37–39].
[37] S. Lee, Y. You, K. Ohkubo, S. Fukuzumi, and W. Nam, Org. Lett. **14**, 2238 (2012).
[38] S. K. Kurtz and T. T. Perry, J. Appl. Phys. **39**, 3798 (1968).
[39] I. Aramburu, J. Ortega, C. L. Folcia, and J. Etxebarria, Appl. Phys. B **116**, 211 (2014).
[40] K. Aizu, Phys. Rev. B **2**, 754 (1970).
[41] W.-Q. Liao, B.-B. Deng, Z.-X. Wang, T.-T. Cheng, Y.-T. Hu, S.-P. Cheng, and R.-G. Xiong, Adv. Sci. **8**, 2102614 (2021).
[42] W.-Q. Liao, Y.-L. Zeng, Y.-Y. Tang, H. Peng, J.-C. Liu, and R.-G. Xiong, J. Am. Chem. Soc. **143**, 21685 (2021).
[43] Z.-X. Wang, C.-R. Huang, J.-C. Liu, Y.-L. Zeng, and R.-G. Xiong, Chem. Eur. J. **27**, 14831 (2021).
[44] Y.-Y. Tang, J.-C. Liu, Y.-L. Zeng, H. Peng, X.-Q. Huang, M.-J. Yang, and R.-G. Xiong, J. Am. Chem. Soc. **143**, 13816 (2021).
[45] Z.-X. Wang, X.-G. Chen, X.-J. Song, Y.-L. Zeng, P.-F. Li, Y.-Y. Tang, W.-Q. Liao, and R.-G. Xiong, Nat. Commun. **13**, 2379 (2022).
[46] Y.-Y. Tang, Y.-L. Zeng, and R.-G. Xiong, J. Am. Chem. Soc. **144**, 8633 (2022).
[47] K. Matsuda, K. Takayama, and M. Irie, Chem. Commun. (Cambridge) **4**, 363 (2001).
[48] Y. Liu, Y. Zhang, M.-J. Chow, Q. N. Chen, and J. Li, Phys. Rev. Lett. **108**, 078103 (2012).